

23 kHz MEMS based swept source for optical coherence tomography imaging

Barry Vuong, Cuiru Sun, Mark K. Harduar, Adrian Mariampillai, Keiji Isamoto, Changho Chong, Beau A. Standish, and Victor X.D. Yang

Abstract—The transition from benchtop to clinical system often requires the medical technology to be robust, portable and accurate. This poses a challenge to current swept source optical coherence tomography imaging systems, as the bulk of the systems footprint is due to laser components. With the recent advancement of micromachining technology, we demonstrate the characterization of a microelectromechanical system (MEMS) swept source laser for optical coherence tomography imaging (OCT). This laser utilizes a 2 degree of freedom MEMS scanning mirror and a diffraction grating, which are arranged in a Littrow configuration. This resulted in a swept source laser that was capable of scanning at 23.165 kHz (bidirectional) or 11.582 kHz (unidirectional). The free spectral range of the laser was ≈ 100 nm with a central wavelength of ≈ 1330 nm. The 6dB roll off depth was measured to be at 2.5 mm. Furthermore, the structural morphology of a human finger and tadpole (*Xenopus laevis*) were evaluated. The overall volumetric footprint of the laser source was measured to be 70 times less than non-MEMS swept sources. Continued work on the miniaturization of OCT system is on going. It is hypothesized that the overall laser size can be reduced for suitable OCT imaging for a point of care application.

I. INTRODUCTION

Swept-source optical coherence tomography (SS-OCT) is a novel, inexpensive and minimally invasive imaging modality that produces a micron-scale spatial resolution (1 - 10 μm) with imaging depths of 1-3 mm [1]. The SS-OCT image formation is based on the measurement of backscattered light as a function of depth. With sequential A-scans acquired, the formation of a 2D cross-sectional image can be resolved, where the contrast of the image is based on the optical backscattering of the tissue [2].

Previous medical applications of SS-OCT range from evaluating the progression of tumors in anatomical sites such as the breast [3], esophagus [4], and prostate to measurement of micro-vasculature blood flow or monitoring treatments [5]. Generally, SS-OCT systems are comprised of a semiconductor gain medium within a fiber ring cavity, where

This work was supported by Natural Science and Engineering Research Council of Canada Strategic Project Grants (NSERC-SPG) and Canada Foundation for Innovation (CFI)

V.X.D Yang is with the Department of Electrical and Computer Engineering, Ryerson University, ON M5B 2K3, Canada, & Division of Neurosurgery, University of Toronto, Toronto, Canada, and Imaging Research, Sunnybrook Health Sciences Center, Toronto, Canada yangv@ee.ryerson.ca

K. Isamoto and C.Chong are with Santec Corporation, Komaki, Aichi 4850802, Japan k.isamoto@santec-net.co.jp and tei3@santec-net.co.jp

B. Vuong, C. Sun, M.K. Harduar, A. Mariampillai, B.A. Standish are with the Department of Electrical and Computer Engineering, Ryerson University, ON M5B 2K3, Canada correspondence to yangv@ee.ryerson.ca

there is a tunable wavelength filter. These tunable wavelength filters can be implemented in variety of techniques such as, a polygon mirror [6], Fabry-perot filter [7], or galvanometer mirror and a diffraction grating to optically filter specific wavelengths [16]. As a result, the narrow range of wavelengths enter the gain medium for amplification.

Unfortunately, the majority of SS-OCT systems require a trained operator, are large, and heavy to be considered as a point of care technology. This may add to the difficulty of achieving wide-spread clinical adoption of SS-OCT systems. Goldberg et al. [8] have recently demonstrated a miniature high-speed swept source laser by utilizing a resonant mirror. The result was a swept source that has similar dimension to a deck of cards for point of care application. However, this miniature laser had an optical output power of 12 mW and a bandwidth of 75 nm centered at 1340 nm, which would affect the signal to noise and imaging resolution, respectively. By developing a robust, lightweight, portable, accurate and inexpensive swept source lasers for OCT imaging, the translation to clinical application is more likely to be adopted.

Over the past two decades, the development of microelectromechanical systems (MEMS) have rapidly advanced. Applications include bar code scanners, displays and imaging devices. Furthermore, MEMS technologies have been demonstrated to provide optical beam steering within an endoscopic probe for OCT imaging [9]. This significant miniaturization of optical components could be adapted to downsize the conventional polygon mirror or galvanometer mirror component of the tuning wavelength filter [10]. As a result, the reduced power consumption and smaller form factor could allow for a small handheld unit.

In this paper we present a high-speed MEMS swept source laser for point of care OCT imaging. The MEMS based laser has an free spectral range of ≈ 100 nm centered at ≈ 1330 nm. The bidirectional scan rate of the laser is 23.165 kHz at a peak optical power of ≈ 36 mW.

II. EXPERIMENTAL SETUP

A. MEMS Swept Source Laser

Figure 1 depicts a two-degree of freedom MEMS mirror in ring cavity configuration. The two degrees of freedom refers to the dual hinges (outer θ_1 and inner θ_2). The outer hinge acts as an anchor and is connected to thick torsion bars, where an actuator plate is connected to the mirror by a thin torsion bar. As the actuator plate oscillates, the motion is translated to the mirror and angle of the mirror is magnified by the anchors. This allows for faster

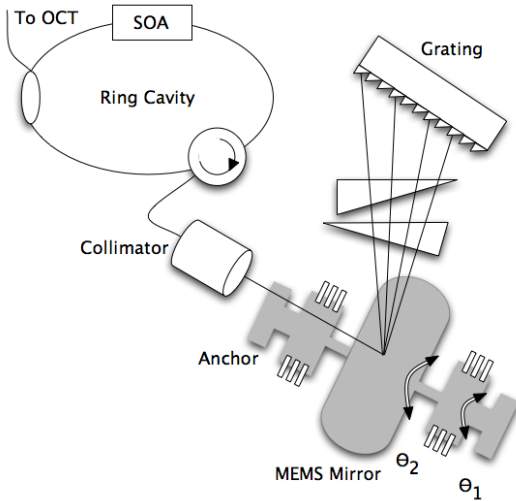


Fig. 1: Simplified Schematic of MEMS swept source laser. The MEMS mirror has 2 degrees of freedom, where outer angular rotation is θ_1 and inner angular rotation is θ_2 .

scanning speed, while maintaining a large reflection angle. As infrared light emitted from the collimator is reflected by the MEMS mirror and is incident upon a 1312 grooves/mm grating. Depending on the angle at which the light interacts with the grating, a narrow wavelength retraces its path back to the collimator. As the mirror resonates along its axis, various narrow bands of light are selected with respect to time. This light becomes amplified by the semiconductor optical amplifier and is propagated to the ring-cavity OCT system. Between the MEMS mirror and grating are a pair of prisms, which act as an expander in the plane parallel to the deflection. This enlarges the beam resulting in a narrower line-width of the swept source. Furthermore, by adjusting the orientation of the prism, insertion loss and chromatic dispersion are reduced [11].

B. Optical Coherence Tomography

A portion of amplified light from the MEMS based ring cavity is used to generate a clock signal for k-space remapping, while the majority of the light is coupled into a fiber beam splitter (Figure 2). Ten percent of the of this light was directed to the reference arm and 90 percent was directed to the sample arm. The interference signal was received by a dual balanced detector (PDB140C, Throlabs) and digitized by an acquisition card (PCI-6731, National Instrument) at 50 Msamples per second. During imaging, two function generators were required. One of the function generators triggered the MEMS driver with a square wave of 23.166 kHz, while the other function generator delayed the MEMS driver signal to trigger the DAQ card, in order to capture a line of data (A-mode). Cubic spline interpolation of the clock and fringe signals were used to re-sample prior to the visualization of the OCT image, which was processed in MATLAB (R2009a, Mathworks).

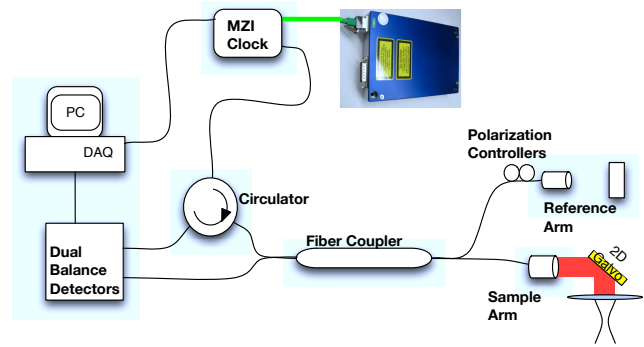


Fig. 2: Simplified Schematic of MEMS-OCT system

C. In vivo imaging

Initial OCT images consisted of imaging a human finger (*in vivo*) placed under a x-y scanning head consisting of a lens (AC254-30-C, Thorlabs) and galvanometers (GVS002, Thorlabs). A tadpole (*xenopus laevis*) was anesthetized in 0.001% lidocaine solution prior to imaging. The specimen was immersed in water on a shallow grooved foam and oriented such that the incident light interrogated the ventral side.

III. RESULTS

A. MEM Swept Source Characteristics

The free spectral range of the laser was measured to be 100 nm with a peak optical power of 35 mW centred at 1330 nm (Figure 3). The dimensions of the MEMS swept source laser were 17 x 11 x 3 cm, which when compared to other non-MEMS swept source sources resulted in a 70 times reduction in volumetric footprint.

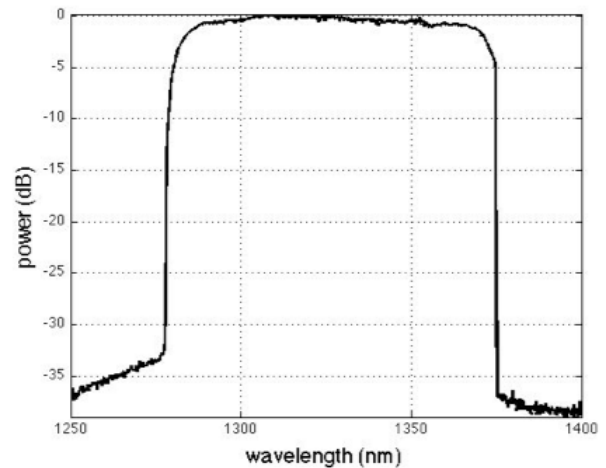


Fig. 3: Spectrum of MEMS Swept Source. The spectral bandwidth of the laser was measured to be 100 nm (free spectral range) with a bi-directional sweeping rate of 23.166 kHz.

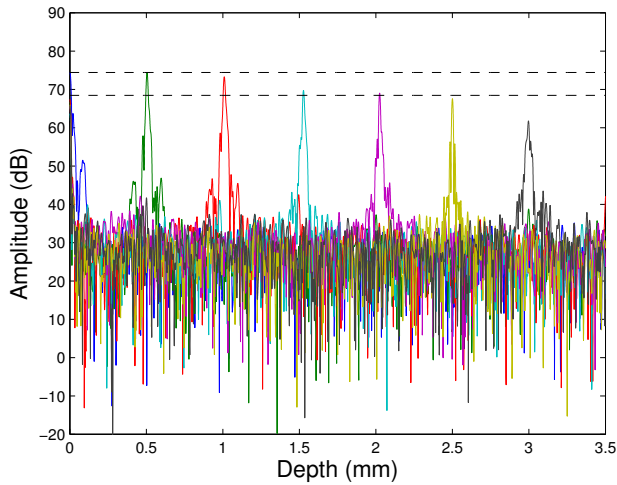


Fig. 4: Measured point spread function (PSF) with respect to depth. This is achieved by translating a gold plated mirror in the sample arm at several depths intervals (0 to 3 mm).

The measurement of the point spread functions (PSF) with respect to depth were characterized by placing a gold plated mirror mounted on a translation stage in the sample arm. The PSF was measured with an 80 MHz detector at several depths intervals (0 to 3 mm). This measurement allows for the calculation of the 6dB roll off of the system along with the identification of potential system dispersion compensation requirements. Figure 4 depicts the PSF measurement and it was observed that the 6dB roll off was 2 mm with a measured axial resolution of $9 \mu\text{m}$.

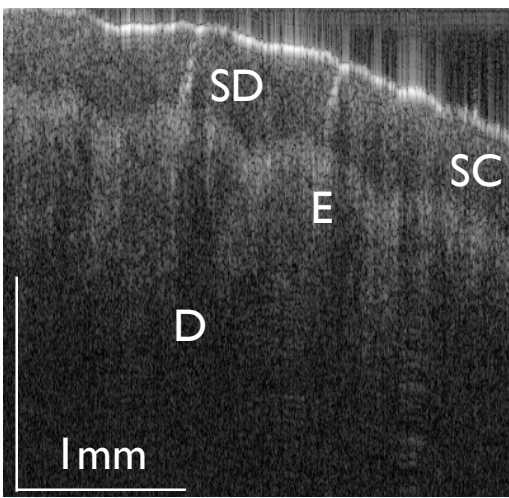


Fig. 5: OCT image of the ventral side of a human finger that is obtained with the MEM swept source laser. The stratum corneum (SC), epidermis (E), dermis (D) and sweat Ducts (SD) can be resolved.

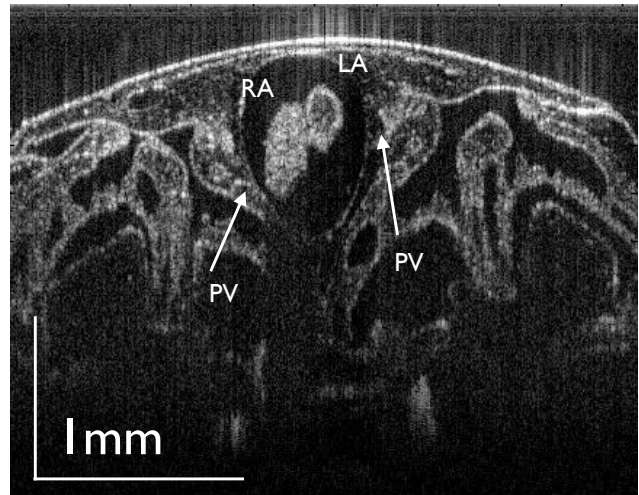


Fig. 6: OCT image of the ventral side of a *Xenopus Laevis* embryo that is obtained with the MEM swept source laser. The right atria (RA), left atria (LA) and (PV) pulmonary gill vessels can be resolved.

B. *In vivo* imaging

In this study, two *in vivo* tissue types were imaged using the MEMS based swept source laser. Figure 5 illustrates a cross sectional OCT image of a human finger tip. It was observed that the MEMS-OCT system had the ability to resolve the stratum corneum, the stratum lucidum and the superficial morphology of the dermis. The spiral structures that were observed in the stratum corneum denotes the presence of sweat ducts.

An axial view of a tadpole was imaged with the MEMS based swept source laser (Figure 6). The tadpole was chosen for this experiment due to its optically transparent surface, during the early stages of development. As a result, the right and left atria are clearly visualized, as well as the pulmonary gill vessels. Surrounding structures of the heart chamber and deeper tissue penetration with respect to the human finger was observed. Both the finger and tadpole OCT images were reconstructed with the forward directional sweep of the laser in order to reduce the signal processing time.

IV. DISCUSSION

The miniaturization of an OCT system can potentially provide physicians and care givers with bedside images near the histological resolution. It was demonstrated that the MEMS swept source has the capability to resolve the morphology of a finger and tadpole, which was similar to previous polygon based swept source when comparing imaging speed, resolution and signal-to-noise ratios [12], [13]. However it was observed in several *in vivo* images, that there was a slight increase in back-reflection at the surface of the tissue compared to other swept source lasers. This abnormality may be due to the inability to optimally compensate for the polarization in the interferometers. Nevertheless, the overall performance of the MEMS swept source laser was promising

in the bench top research environment. For future imaging, it would be beneficial to have sweeping rates $>23\text{kHz}$ during a surgical procedure in order to ascertain volumetric data and suppress motion artifacts. In the development of MEMS resonant mirror, there are design limitations that result in a tradeoff between the repetition speed and resolution of the image. Attempts to increase the sweeping rate would result in a decrease in bandwidth, which in turn decreases the axial resolution of the system.

Another clinical tool, which could be beneficial to the physician is the functional extension of OCT to include blood flow detection or Doppler-OCT (DOCT). DOCT allows for analysis of imaging of non-stationary particles, where this technique has been applied to various experiments such as photodynamic therapy for cancer treatment [4], fluid dynamics of interstitial blood flow [14], microvascular visualization [15], and retinal blood flow [16]. The ability to measure the movement of particles is dependent on the phase characteristics of the swept source laser. Unfortunately, due to the sub-optimal triggering by the external function generators, the phase characteristics of the swept source laser could not be accurately obtained. Linearly sweep in k-space trigger will simplify the image reconstruction algorithm, as the resampling of k-space will no longer be required, and will facilitate Doppler measurement [7], [17].

While the MEMS swept source laser had a dramatic size reduction, the current size of the entire OCT system is still not ideal for point of care. A true MEMS-OCT system for point of care application requires not only the swept source to be small and portable, but also the interferometer, photodetectors, scanning mechanism, the display, and DAQ [8]. However, the size of the swept source is not the only limiting factor. Previous studies have demonstrated the design of optical fiber based probes for interstitial imaging at various anatomical locations. This approach is advantageous due to the size of optical fiber, where it is possible to incorporate them into surgical tools such as, endoscope, aspiration needles, and guide-wires. As a result, these probes can be designed to overcome the 3 mm penetration depth of OCT. Further reduction in size can be achieved by removing the bulk optics in the interferometer along with the utilization of embedded digital signal processors rather than external data acquisition cards.

V. CONCLUSION

In this paper, we have provided the laser characteristics of a MEMS swept source laser suitable for point-of-care imaging. The size of the overall laser is 70 times smaller than non-MEMS polygon swept source system and can achieve a peak output power of 35mW with a tuning bandwidth of 100 nm at a bidirectional tuning rate of 23.166 kHz.

VI. ACKNOWLEDGMENTS

The authors gratefully acknowledge the contribution of Natural Science and Engineering Research Council of Canada Strategic Project Grants (NSERC-SPG) and Canada Foundation for Innovation (CFI).

REFERENCES

- [1] S. Yun, G. Tearney, J. de Boer, N. Ifimia, and B. Bouma, "High-speed optical frequency-domain imaging," *Optics Express*, vol. 11, no. 22, pp. 2953–2963, 2003.
- [2] F. Van der Meer, D. Faber, D. Sassoon, M. Aalders, G. Pasterkamp, T. Van Leeuwen, L. Center, M. Center, and N. Amsterdam, "Localized measurement of optical attenuation coefficients of atherosclerotic plaque constituents by quantitative optical coherence tomography," *IEEE transactions on medical imaging*, vol. 24, no. 10, pp. 1369–1376, 2005.
- [3] F. Nguyen, A. Zysk, E. Chaney, J. Kotynek, U. Oliphant, F. Bellafiore, K. Rowland, P. Johnson, and S. Boppart, "Intraoperative evaluation of breast tumor margins with optical coherence tomography," *Cancer research*, vol. 69, no. 22, p. 8790, 2009.
- [4] B. Standish, V. Yang, N. Munce, L. Wong Kee Song, G. Gardiner, A. Lin, Y. Mao, A. Vitkin, N. Marcon, and B. Wilson, "Doppler optical coherence tomography monitoring of microvascular tissue response during photodynamic therapy in an animal model of Barrett's esophagus," *Gastrointestinal Endoscopy*, vol. 66, no. 2, pp. 326–333, 2007.
- [5] A. Mariampillai, B. Standish, E. Moriyama, M. Khurana, N. Munce, M. Leung, J. Jiang, A. Cable, B. Wilson, I. Vitkin *et al.*, "Speckle variance detection of microvasculature using swept-source optical coherence tomography," *Optics letters*, vol. 33, no. 13, pp. 1530–1532, 2008.
- [6] W. Oh, S. Yun, G. Tearney, and B. Bouma, "115 kHz tuning repetition rate ultrahigh-speed wavelength-swept semiconductor laser," *Optics letters*, vol. 30, no. 23, p. 3159, 2005.
- [7] R. Huber, M. Wojtkowski, K. Taira, J. Fujimoto, and K. Hsu, "Amplified, frequency swept lasers for frequency domain reflectometry and OCT imaging: design and scaling principles," *Optics Express*, vol. 13, no. 9, pp. 3513–3528, 2005.
- [8] B. Goldberg, S. Motaghian Nezam, P. Jillella, B. Bouma, and G. Tearney, "Miniature swept source for point of care optical frequency domain imaging," *Optics express*, vol. 17, no. 5, pp. 3619–3629, 2009.
- [9] Y. Pan, H. Xie, and G. Fedder, "Endoscopic optical coherence tomography based on a microelectromechanical mirror," *Optics Letters*, vol. 26, no. 24, pp. 1966–1968, 2001.
- [10] K. Totsuka, K. Isamoto, T. Sakai, A. Morosawa, and C. Chong, "MEMS scanner based swept source laser for optical coherence tomography," in *Proceedings of SPIE*, vol. 7554, 2010, p. 75542Q.
- [11] C. Chong, A. Morosawa, and T. Sakai, "High-speed wavelength-swept laser source with high-linearity sweep for optical coherence tomography," *Selected Topics in Quantum Electronics, IEEE Journal of*, vol. 14, no. 1, pp. 235–242, 2008.
- [12] N. Ifimia, B. Bouma, J. De Boer, B. Park, B. Cense, and G. Tearney, "Adaptive ranging for optical coherence tomography," *Optics express*, vol. 12, no. 17, p. 4025, 2004.
- [13] A. Mariampillai, B. Standish, . Randall, G. Liu, N. Munce, I. Vitkin, A. Cable, J. Jiang, and V. Yang, "Optical cardiogram gated 2d doppler flow imaging at 1000 fps and 4d imaging at 36 fps on a swept source oct system," *Opt. Express*, vol. 15, pp. 1627–1638, 2007.
- [14] B. Vakoc, R. Lanning, J. Tyrrell, T. Padera, L. Bartlett, T. Stylianopoulos, L. Munn, G. Tearney, D. Fukumura, R. Jain *et al.*, "Three-dimensional microscopy of the tumor microenvironment in vivo using optical frequency domain imaging," *Nature medicine*, vol. 15, no. 10, pp. 1219–1223, 2009.
- [15] B. White, M. Pierce, N. Nassif, B. Cense, B. Park, G. Tearney, B. Bouma, T. Chen, and J. de Boer, "In vivo dynamic human retinal blood flow imaging using ultra-high-speed spectral domain optical coherence tomography," *Optics Express*, vol. 11, no. 25, pp. 3490–3497, 2003.
- [16] V. Srinivasan, R. Huber, I. Gorczynska, J. Fujimoto, J. Jiang, P. Reisen, and A. Cable, "High-speed, high-resolution optical coherence tomography retinal imaging with a frequency-swept laser at 850 nm," *Optics letters*, vol. 32, no. 4, pp. 361–363, 2007.
- [17] S. Vergnole, D. Lévesque, and G. Lamouche, "Experimental validation of an optimized signal processing method to handle non-linearity in swept-source optical coherence tomography," *Optics Express*, vol. 18, no. 10, pp. 10446–10461, 2010.